ROM SAF Report 29
Ref: SAF/ROM/METO/REP/RSR/029
Web: www.romsaf.org
Date: 4 April 2017

The EUMETSAT Network of Satellite Application Facilities

ROM SAF
Radio Occultation Meteorology

ROM SAF Report 29

Testing reprocessed GPS radio occultation datasets in a reanalysis system

Sean Healy and Andras Horanyi

ECMWF

Document Author Table

	Name	Function	Date	Comments
Prepared by:	S. Healy	ROM SAF Project Team	4 April 2017	
Reviewed by:	C. Burrows	ROM SAF Project Team	20 March 2017	
Reviewed by:	-	-	-	
Approved by:	K. B. Lauritsen	ROM SAF Project Manager	4 April 2017	

Document Change Record

Issue/Revision	Date	By	Description
0.1	20 March, 2017	S. Healy	Draft for review.
1.0	4 April, 2017	S. Healy	Official release after review.

ROM SAF

The Radio Occultation Meteorology Satellite Application Facility (ROM SAF) is a decentralised processing centre under EUMETSAT which is responsible for operational processing of GRAS radio occultation data from the Metop satellites and RO data from other missions. The ROM SAF delivers bending angle, refractivity, temperature, pressure, and humidity profiles in near-real time and offline for NWP and climate users. The offline profiles are further processed into climate products consisting of gridded monthly zonal means of bending angle, refractivity, temperature, humidity, and geopotential heights together with error descriptions.

The ROM SAF also maintains the Radio Occultation Processing Package (ROPP) which contains software modules that will aid users wishing to process, quality-control and assimilate radio occultation data from any radio occultation mission into NWP and other models.

The ROM SAF Leading Entity is the Danish Meteorological Institute (DMI), with Cooperating Entities: i) European Centre for Medium-Range Weather Forecasts (ECMWF) in Reading, United Kingdom, ii) Institut D'Estudis Espacials de Catalunya (IEEC) in Barcelona, Spain, and iii) Met Office in Exeter, United Kingdom. To get access to our products or to read more about the project please go to: http://www.romsaf.org

Intellectual Property Rights

Abstract

The ROM SAF plans to run two long GPS radio occultation (GPS-RO) reanalyses for the period 2007-2015. Temporal averaging of the gridded, three-dimensional reanalysis fields is an alternative way of producing level-3 climatologies based on GPS-RO data. In preparation for this activity, a series of experiments have been performed using the ERA5 reanalysis system. The experiments assimilate reprocessed GPS-RO datasets from both UCAR and the ROM SAF, and the operational GPS-RO data from the period. The impact of a subset of other measurement types has also been tested. We have found that the mean bending departure differences between the GPS-RO datasets in the vertical interval between $\sim$ 10-30 km are around 0.1 %, which is about a tenth of the assumed measurement/forward model uncertainty. Consequently, the zonally averaged temperatures computed from the reanalyses are reasonably consistent below 5 hPa. We have also found that assimilating AMSU-A channel 14 radiances without bias correction is crucial for correcting large model biases around 2 hPa. Furthermore, these model biases appear to be in the GPS-RO null-space. Therefore, we conclude that AMSU-A channel 14 should be included in both of the proposed ROM SAF reanalyses.

It is noted that one internal (non public) ROM SAF dataset has poorer bending angle departure statistics, because quality control flags are not set correctly, but this is resolved in the later dataset. The ROM SAF data numbers tend to be lower than the operational GRAS data from the period. The reasons are understood and they will be resolved in the official version 1 (V1.0) of the ROM SAF Climate Data Record (CDR V1.0) reprocessing.

Contents

1 Introduction and Main Results **5**
1.1 Introduction 5
1.2 Reanalysis Experiments 6
1.3 Main results 7

2 Summary and Future Work **20**

1 Introduction and Main Results

1.1 Introduction

GPS radio occultation (GPS-RO) measurements complement satellite radiances because they have good vertical resolution, and they do not require bias correction. This is because the raw GPS-RO observables are time-delays and they are measured with an atomic clock (Kursinski *et al.*, 1997). It has been demonstrated that GPS-RO measurements provide accurate temperature information in the vertical interval from around 10 km to 35 km ($\sim$ 250 hPa to 5 hPa), and they have become an important observation type for numerical weather prediction (NWP) applications (Healy and Thépaut 2006; Cucurull *et al.*, 2007; Aparicio and Deblonde 2008; Poli *et al.*, 2009; Rennie 2010). The measurements are also likely to become increasingly important for climate applications as the time series lengthens. For example, the impact of GPS-RO in climate reanalyses has been investigated by Poli *et al.*, (2010), and a number of studies outlining climate monitoring applications have been reported (e.g., Leroy *et al.*, 2006). In addition, in the"RoTrends project", the major GPS-RO processing centres process common datasets in order to estimate structural uncertainty in their GPS-RO geophysical retrievals (e.g., Steiner *et al.*, 2013).

It should be recognised that GPS-RO observations are not direct measurements of geophysical quantities, such as temperature, pressure and humidity, and that a retrieval scheme is required to map from the raw observables to the geophysical quantities (e.g. see Kursinski et al (1997). The GPS-RO retrieval is ill-posed and therefore it introduces *a priori* information through the processing steps such as "statistical optimization" (Healy, 2001), and the initialisation of the hydrostatic integration (Kursinski *et al.*, 1997). Although some recent work has been done on propagating average bending angle profiles through retrieval schemes, in order to reduce the impact of the *a priori* information (Ao *et al.*, 2012; Gleisner and Healy, 2013), and Leroy *et al.* (2012) have suggested climatologies based on Bayesian interpolation techniques, most monthly and seasonal GPS-RO climatologies are still computed by binning and averaging individual geophysical retrievals. Clearly, these will have some sensitivity to the *a priori* information used in the retrievals, and this probably accounts for why the various GPS-RO climatology differences tend to increase when mapping from bending angles, to refractivity and subsequently the geophysical quantities.

An alternative approach for generating monthly and seasonal climatologies is based on assimilating GPS-RO data, and possibly a subset of other observations, into a climate reanalysis system. A four-dimensional variational assimilation system (4D-Var) (Rabier *et al.*, 2000) tries to fit all of the observed data in a 12 hour assimilation window and produce a statistically optimal three-dimensional, gridded analysis of the geophysical variables. The 4D-Var system can be viewed as a large geophysical retrieval scheme, which simultaneously retrieves information from multiple observations. Two 4D-Var analyses are produced per day, at 00Z and 12Z. Hence, monthly and seasonal climatologies can be produced by averaging these analyses over the required periods. This is similar to the Bayesian interpolation approach (Leroy *et al.*, 2012) but in our reanalysis system approach, the statistical

interpolator is replaced with an NWP forecast model.

The ROM SAF aims to produce two, three-dimensional gridded climatologies based on climate reanalyses. These will be available to users, but they will not formally be a ROM SAF product. It has been proposed that one climatology will be based on just assimilating GPS-RO into the reanalysis system, and the other will be based on assimilating GPS-RO, plus a subset of other data that can be assimilated without bias correction. Measurements that can be assimilated without bias correction are known as “anchor observations”.

The two ROM SAF reanalyses spanning the period 2007-2015 will be described in detail in a later report. This report focuses on the sensitivity of the reanalysis results to different GPS-RO datasets valid for the same period, and to the choice of the other anchor measurements, such as the inclusion of AMSU-A channel 14. The main aim of this work is to select datasets for use in the two forthcoming ROM SAF reanalyses. We do not report on reprocessed data produced by EUMETSAT here. A reprocessed GRAS geometrical optics (GO) dataset was provided to ECMWF, and tested without any obvious problems. However, this data included a “radius of curvature error”, found subsequently by Stig Syndergaard (DMI) in 2016, and consequently the results will not be shown here. Corrected EUMETSAT reprocessed datasets, now based on wave optics (WO) for Metop-A/B GRAS, COSMIC and CHAMP, will be delivered in 2017 (Joerg Schultz, EUMETSAT, pers. comm. 2017).

In section 1.2, we outline the main experiments. The results are summarised in section 1.3 and a summary of the work is given in section 2.

1.2 Reanalysis Experiments

The experiments cover the six month period from January 1, 2011 to June 30, 2011. The period was chosen based on the availability of the various datasets. They use the Integrated Forecast System (IFS) branch currently used for the Copernicus ERA-5 reanalysis (see https://climate.copernicus.eu/climate-reanalysis). One difference is that the background uncertainty estimates used in this study are static, because they are not produced with an ensemble of data assimiltions (EDA). In practice, the EDA only contributes about 15 % variability to the total background error covariance, and it is unlikely to have a major impact on monthly and seasonal averages. In addition, the experiments shown here are performed at lower resolution than ERA-5, with a 4D-Var outer loop of T159 ($\sim$ 125 km horizontal sampling).

The GPS-RO data are assimilated with the two-dimensional bending angle operator used operationally at ECMWF, but this is unlikely to have any significant impact at T159. The assumed GPS-RO error covariance matrix, $\mathbf{R}$, is a global model, and vertical error correlations are not included. The percentage bending angle errors are given as a function of impact height, h, which is defined as impact parameter minus radius of curvature ($a - r_c$). They fall linearly from 20 $\%$ at h=0, to 1% at h=10 km. The errors above 10 km are then 1% until this reaches a lower absolute limit of 3 microradians. The bending angles are not assimilated above h=50 km because the signal to noise ratio is low. All other observation types are treated in the same way as they are in the ERA-5 reanalysis.

The reanalysis experiments performed in this study include the following:

1. **CTL**: The control experiment, assimilating all the data which is currently used in the

ERA-5 reanalysis. This includes reprocessed COSMIC, GRACE-A, CHAMP and TerraSAR-X data reprocessed by UCAR. Metop-A GRAS is the operational data from this period.

2. **NoRO**: The CTL experiment, but removing all GPS-RO data.
3. **REF**: The CTL experiment, but removing all satellite radiances and all aircraft temperature measurements. The GPS-RO measurements are the reprocessed data used in the CTL experiment and ERA-5 reanalysis.
4. **OPS**: The REF experiment, but using the operational GPS-RO data available at the time, rather than the reprocessed data provided by UCAR.
5. **SAF1**: The REF experiment, but using ROM SAF Metop-A GRAS and COSMIC **Climate Data Record (CDR) test datasets** produced specifically for the present study, using a test version of the reprocessing system running in late 2015, but with incorrect quality control flags.
6. **SAF2**: The REF experiment, but using **ROM SAF CDR Version 0** Metop-A GRAS and COSMIC data produced in summer 2016. This sets the bending angle quality control flags correctly (see below for details).
7. **AMSUA**: The REF experiment but also assimilating channel 14 of AMSU-A as an anchor measurement without bias correction, to constrain the upper stratosphere. This channel peaks near 2 hPa.

1.3 Main results

Given that the aim of this work is to derive monthly and seasonal climate averages from the GPS-RO data, we are mainly concerned with the mean state and the differences in bending angle departure statistics from the various GPS-RO datasets.

The (CTL - NoRO) differences highlight where the GPS-RO measurements are having a significant impact in the full reanalysis system. The zonally averaged (CTL - NoRO) temperature analysis differences are shown in Figure 1.1. In general, the GPS-RO measurements warm the interval between 200-10 hPa by more than 0.1 K. For example, on the 100 hPa level, the spatially averaged temperature difference is $\sim$ 0.3 K. Comparisons with radiosondes indicate that the short-range forecasts are biased cold in the 200-10 hPa interval, so the GPS-RO measurements are trying to reduce this bias. In fact, the temperature biases with respect to radiosonde measurements are improved by $\sim$ 0.1 K in the 200 - 10 hPa interval as result of assimilating the GPS-RO data (Figure not shown). The largest zonally averaged (CTL - NoRO) temperature analysis differences are above 10 hPa. The GPS-RO measurements warm the 2 hPa pressure level by an average of +1.7 K, and cool the 5 hPa level by -2 K on average. These results are consistent with recent testing of the ERA5 reanalysis system, which has shown significant stratospheric temperature biases, prior to the availability of large numbers of GPS-RO measurements with introduction of COSMIC measurements in December 2006. It is also interesting to note that the GPS-RO impact is clear at 2 hPa ($\sim$ 42 km), where there has been a consistent (o-b) bias in operational GPS-RO departure statistics for all instruments. The biases are smaller at 1 hPa, but this is probably because the weight given to the GPS-RO falls with height, and the bending angles are not assimilated above 50 km. At 1 hPa ($\sim$ 48 km), a bending angle value will be typically $\sim$ 20

microradians, and the assumed bending angle uncertainty, σ_o, is 3 microradians. Additional experiments could be performed to assess the impact of the bending angles above 50 km on the mean state, but it should be noted that the measured bending angle values near 60 km are typically only 5 microradians.

Figure 1.2 shows the zonally averaged temperature analysis differences for (CTL-REF), clearly illustrating the impact of the satellite radiance information on the mean temperatures in the stratosphere. Note the difference in contour scales between Figure 1.1 and Figure 1.2. The radiances warm the stratosphere in the northern high latitudes, but more generally the signal is cooling above 5 hPa, with the largest cooling in the southern polar region. In ERA5, all satellite radiances are bias corrected apart from AMSU-A channel 14 (channel 14 hereafter), which has a broad weighting function that peaks near 2 hPa. Channel 14 is correcting an underlying warm model bias in the upper stratosphere, which can lead to particularly large positive temperature ($\sim$ 20 K) biases over the south hemisphere winter pole. This model bias is thought to be caused by the dynamically driven downwelling over the poles being too strong in the model (I. Polichtchouk 2017, presentation at ECMWF, Jan. 11, 2017). Consequently, we find that most of the temperature differences shown in Figure 1.2 can be attributed to channel 14 constraining this particular model bias. This is illustrated in Figure 1.3, which shows the (CTL-AMSUA) temperature differences where only the channel 14 radiances have been added to the standard REF configuration, noting the different temperature scale when compared with Figure 1.2.

Figures 1.1 and 1.2 also illustrate that the GPS-RO measurements and channel 14 radiances provide complementary information in the reanalysis system. The vertical bias pattern shown in Figure 1.1 will be difficult to constrain with channel 14, because it will cancel out when vertically integrated over the channel's weighting function. Conversely, the bias pattern shown in Figure 1.2 will be difficult for GPS-RO to constrain because of a combination of the shape of the bias pattern, and the gradual reduction in GPS-RO signal to noise with height. For example, Figure 1.4 shows the profile of the mean (AMSUA-REF) temperature differences for Antarctica, and it clearly demonstrates the impact of channel 14. The temperature difference at 1 hPa is greater than 8 K, but this only translates to a change in the bending angle departures of $\sim$ 0.6 microradians ((O-B)/B $\sim$ 3 %) at this level, although the bending angle bias is apparent for all instruments. For comparison, to put the 0.6 microradian bias in context, the assumed GPS-RO measurement uncertainty is 3 microradians above $\sim$ 35 km. In general, the GPS-RO measurements can have poor sensitivity to model temperature biases which grow gradually with height, particularly if they do not change the density as a function of height significantly. This is the GPS-RO "null-space", and it is a fundamental limitation of the measurement irrespective of the specific retrieval technique applied. Overall, Figures 1.1 and 1.2 clearly illustrate the benefit of deriving climatologies from from multiple observation types. They also indicate that AMSU-A channel 14 should be included as an anchor measurement in the ROM SAF reanalyses.

Comparing the REF and OPS experiments illustrates the impact of using reprocessed GPS-RO measurements in the reanalysis. Figure 1.5 is fairly typical of the difference in the COSMIC reprocessed and operational departure statistics. The results are for COSMIC-6 rising measurements in the southern hemisphere. The mean departures do not change significantly. The standard deviation of the reprocessed data departures (black lines) are improved above 20 km. The kink at 20 km is related to the transition between geometric optics processing and wave optics processing at this height. In the reprocessed data the

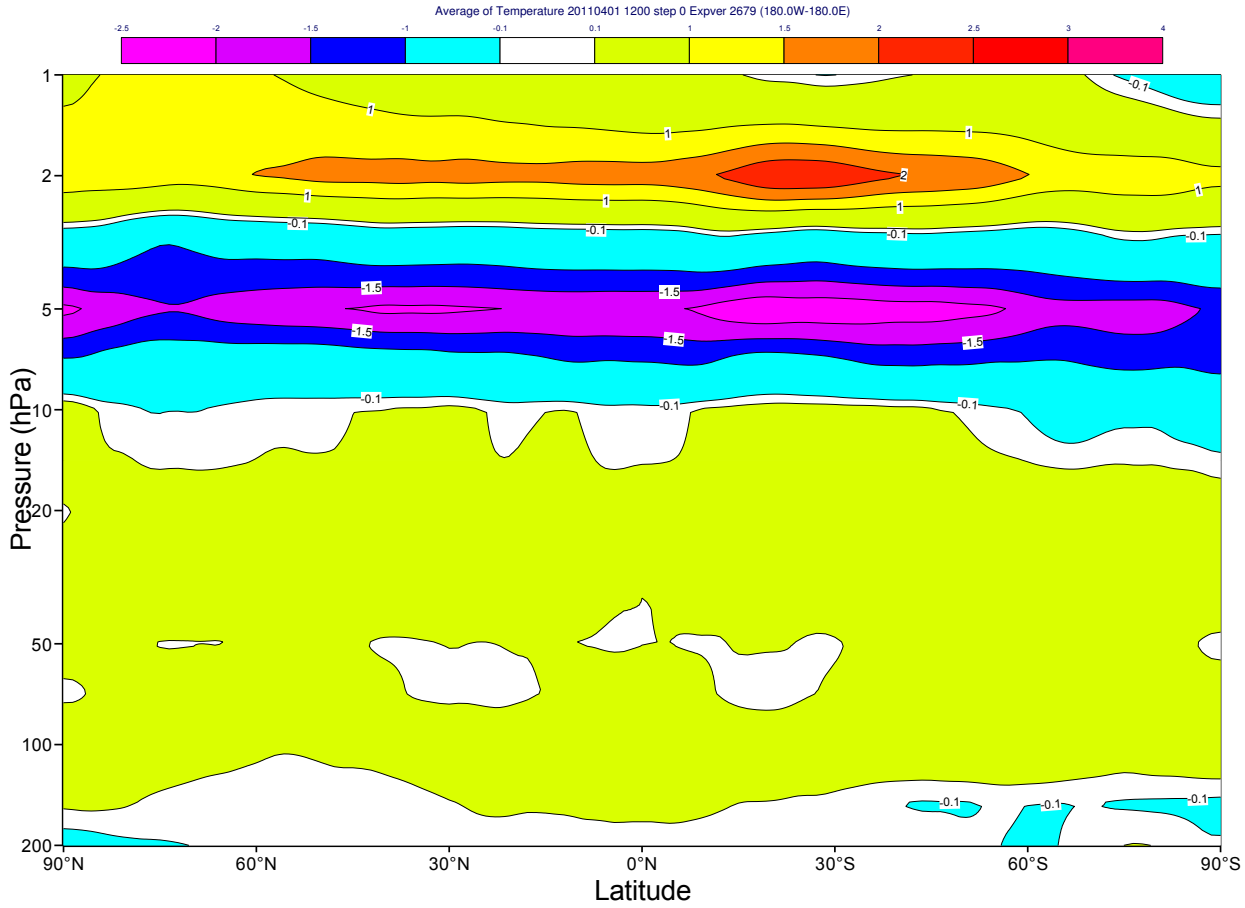

Figure 1.1: The zonally averaged (CTL-NoRO) temperature analysis differences from 200 hPa to 1 hPa. The statistics are averaged over the period April 1 to May 30, 2011.

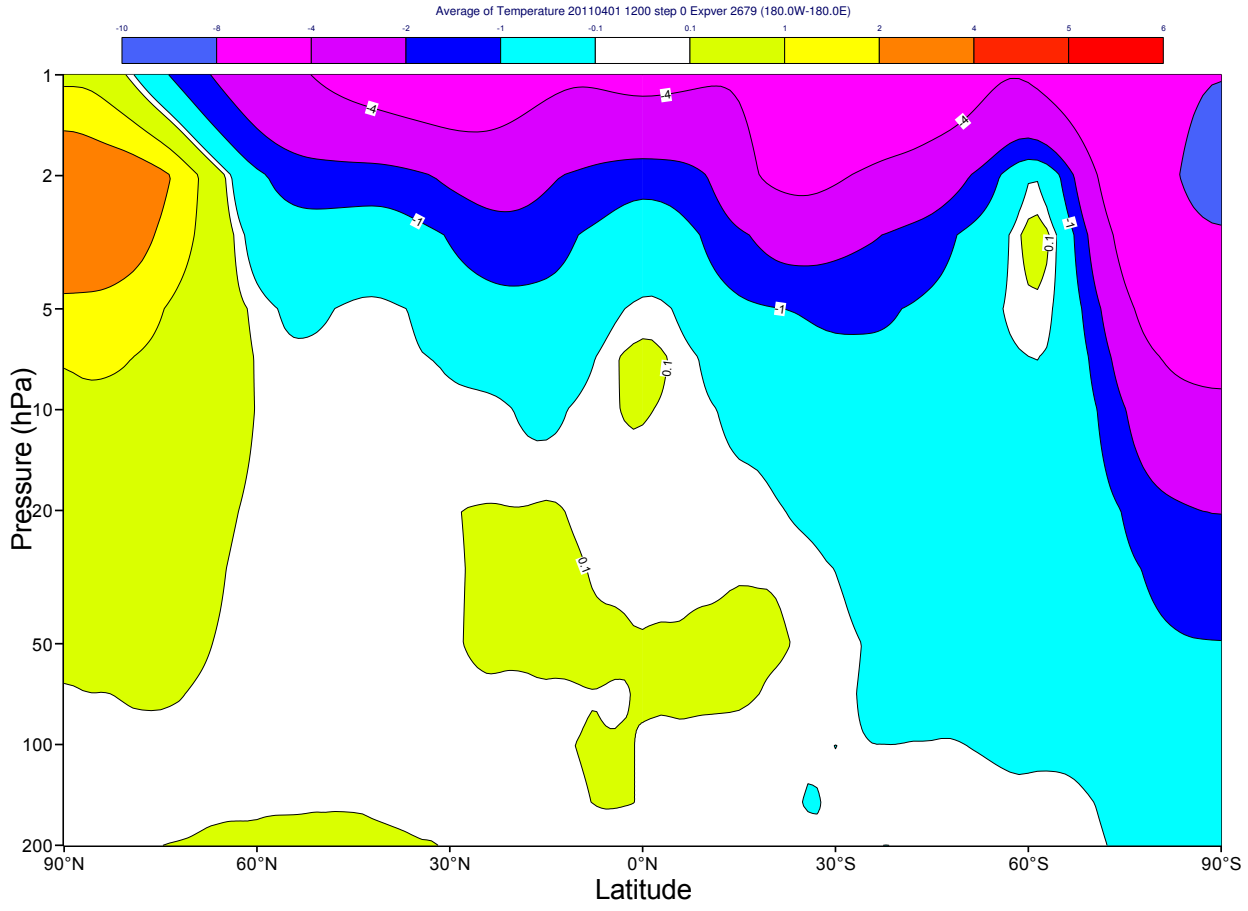

Figure 1.2: The zonally averaged (CTL-REF) temperature analysis differences from 200 hPa to 1 hPa. The statistics are averaged over the period April 1 to May 30, 2011. Note that the contour range highlights the large biases above 10 hPa.

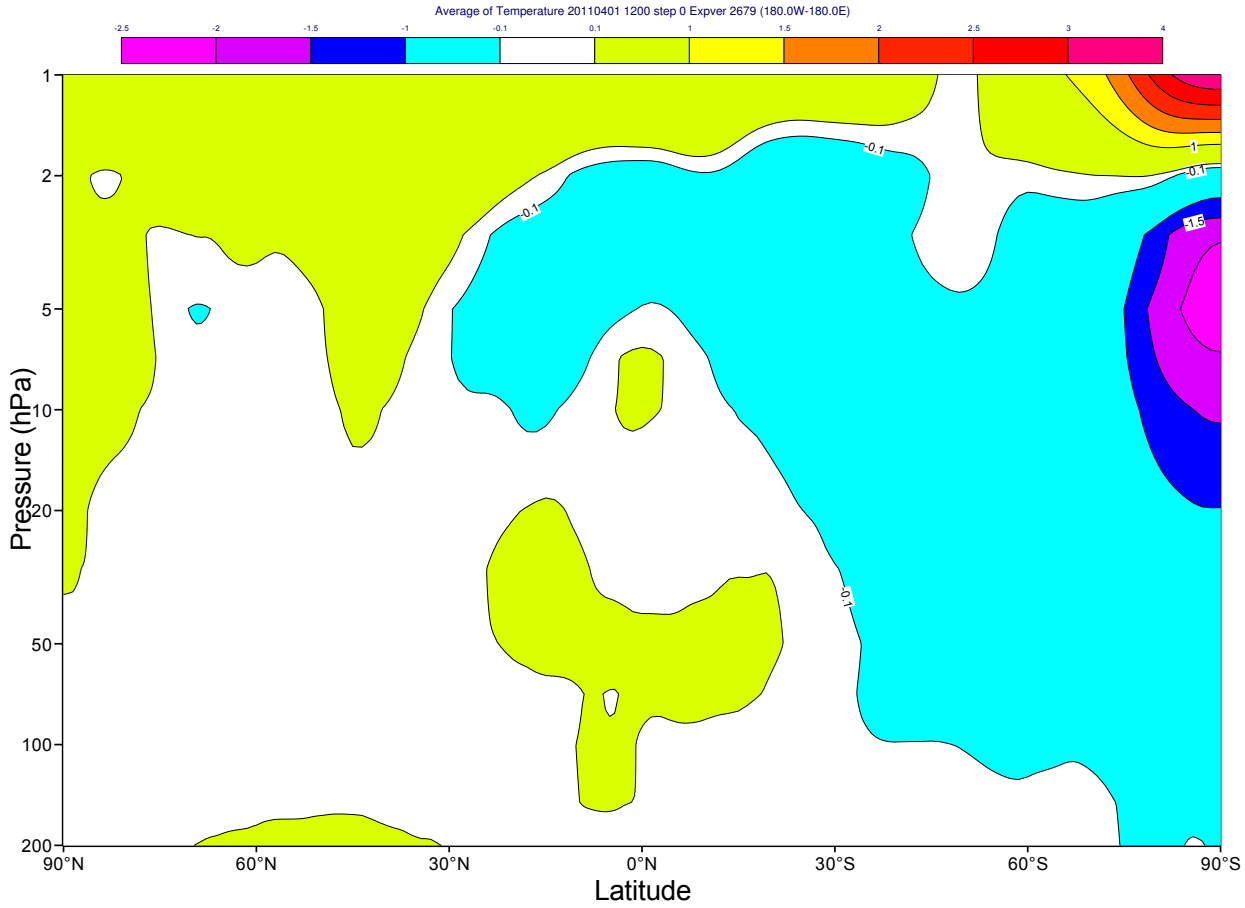

Figure 1.3: The zonally averaged (CTL-AMSUA) temperature analysis differences from 200 hPa to 1 hPa. The statistics are averaged over the period April 1 to May 30, 2011.

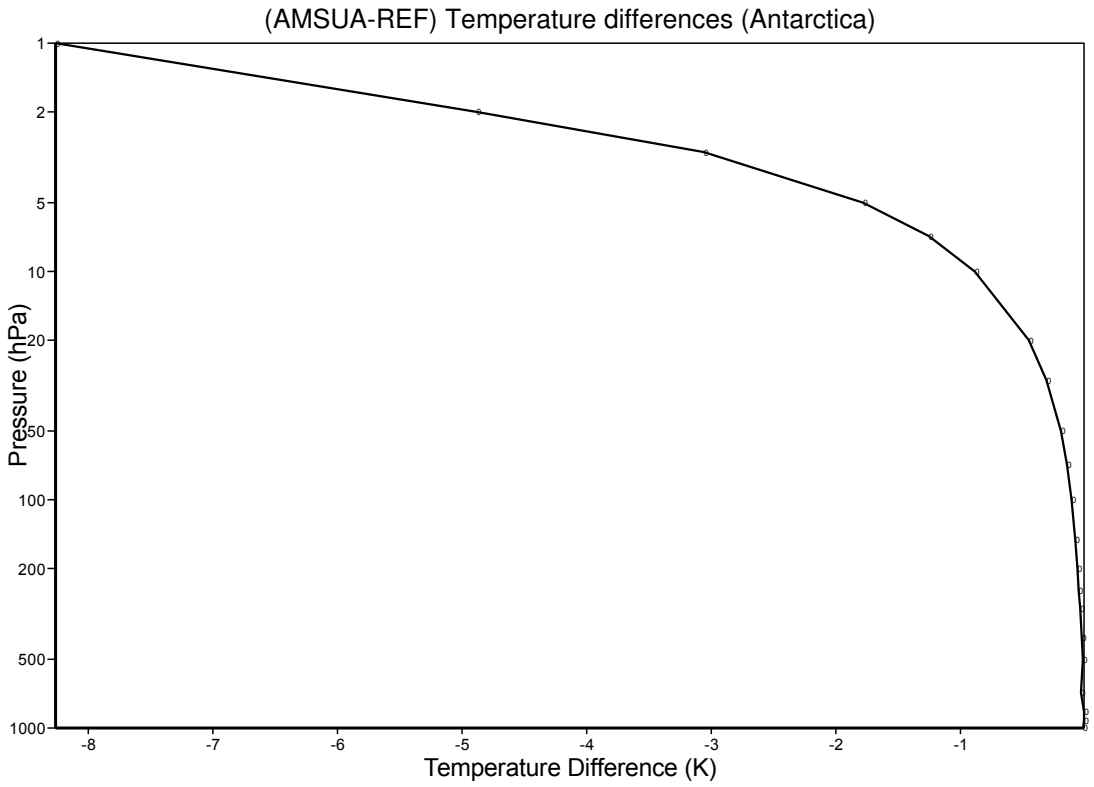

Figure 1.4: The profile of mean (AMSUA-REF) temperature analysis differences for the southern hemisphere polar region (latitude < -65).

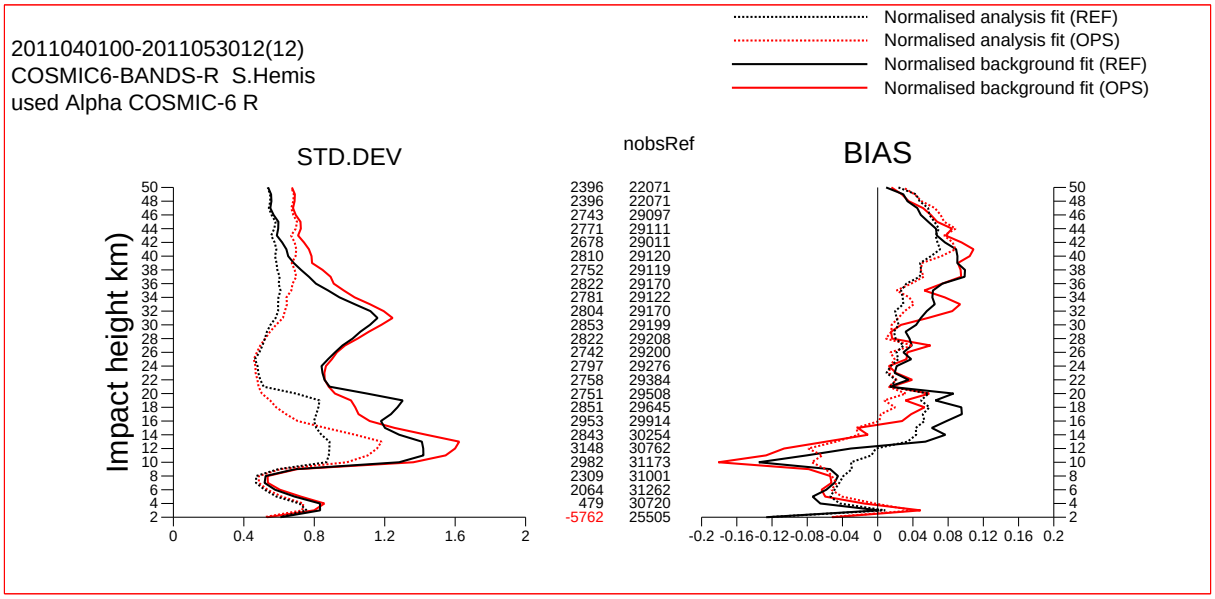

Figure 1.5: The noise normalised forecast and analysis departure statistics ((o-b)/σ_o and (o-a)/σ_o) for COSMIC-6 rising measurements in the southern hemisphere, for the REF (black line) and OPS (red line) experiments. The statistics are computed for the period April 1 to May 30, 2011. The central columns give the data numbers.

transition height is fixed, but in the operational data this height is set dynamically. The data numbers are around $\sim$ 10 % higher in the reprocessed dataset, as would be expected. It should also be noted that the reprocessed CHAMP, GRACE-A and TerraSAR-X provided by UCAR give bending angles up to 60 km, whereas the corresponding operational bending angle profiles provided by GFZ stop at 40 km in this period.

The zonally averaged (REF-OPS) temperature differences are shown in Figure 1.6. In general, the globally averaged mean temperatures differences on the pressure levels below 10 hPa are less than 0.05 K, although the zonally averaged differences can be larger (Figure 1.6). We emphasise that the temperature differences above 10 hPa are relatively small when compared to the (AMSU-REF) or (CTL-REF) differences. More specifically, the bending angle differences have no significant impact on the southern hemisphere polar biases shown in Figure 1.4.

Figure 1.7 shows the bending angle departure statistics for the COSMIC-6 rising measurements in the southern hemisphere for the REF and SAF1 experiments. The discontinuity in the standard deviations in the ROM SAF departures near 25 km is because of the transition between wave-optics and geometrical optics processing, similar to the discontinuity in the reprocessed UCAR data near 20 km. In addition, the ROM SAF data have much poorer departure statistics below 10 km. This problem has been traced to not setting the quality control flags correctly in the *test version* of the ROM SAF processing used in the SAF1 experiment. However, the problem is solved in the ROM SAF data used in SAF2, as illustrated in Figure 1.8. The discontinuity in the standard deviations near 25 km is also removed because additional vertical smoothing is employed in the SAF2 data. The data numbers shown in the central columns in Figure 1.7 and 1.8 indicate that the ROM SAF data numbers are lower. This is slightly misleading because these numbers refer to bending angles in 1 km

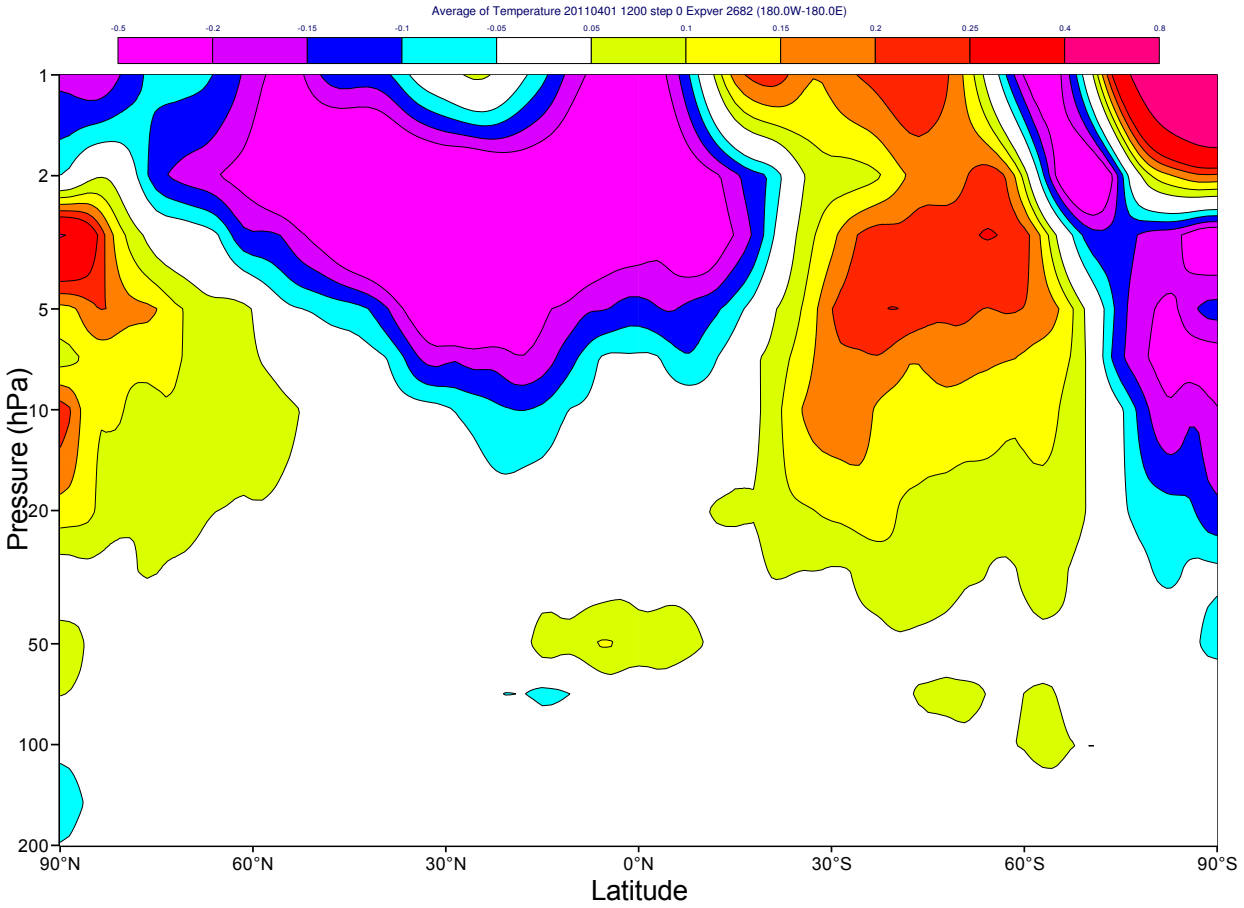

Figure 1.6: The zonally averaged (REF-OPS) temperature analysis differences from 200 hPa to 1 hPa. The statistics are averaged over the period April 1 to May 30, 2011.

bins. UCAR provide data on 300 levels between the surface and 60 km, whereas the SAF provides data in 247 levels in the same vertical interval.

Figures 1.9 and 1.10 show the setting and rising GRAS bending angle departure statistics, respectively, for the REF (black) and SAF2 (red) experiments, noting that REF experiment uses the operational GRAS data from the period. The SAF2 data generally have smaller standard deviations, but this is partly related to broader vertical smoothing used in the SAF2 processing than in the operational data, and it does not necessarily imply a higher information content. The biases in the vertical interval between 10 - 30 km show differences of $\sim 0.1\%$, which is comparable to forward model biases introduced by uncertainty in the refractivity coefficients, for example (e.g., Healy 2011). The basic shape of the bias curves is similar, and it is probably related to the cold bias in the stratospheric temperature forecasts. The data numbers are still lower for the SAF2 data, even though the reprocessed and operational GRAS data are on the same 247 level grid. DMI (Hans Gleisner, pers. comm. 2017) have noted the following issues with "version 0" of the reprocessing system used for the SAF2 dataset, which have reduced data numbers:

1. Profiles are not processed if the 1D-Var refractivity retrieval fails.
2. Profiles can be rejected as a result of a poor statistical optimization fit.
3. Profiles can be rejected as a result of a poor L2 fit.

These problems will be solved in the official ROM SAF CDR V1.0 release of the reprocessed data.

Figure 1.11 shows the (REF-SAF2) differences on the mean temperatures. In general, the (REF-SAF2) difference are largest above 5 hPa, and they have a similar pattern to the (REF-OPS) shown in Figure 1.6. In general, the SAF2 COSMIC bending angle biases seem to be more consistent with the operational data than the reprocessed COSMIC data used in the REF experiment. However, it is important to recognise that these differences are quite small compared to the impact of channel 14 radiances above 5 hPa. The temperature differences near 70 hPa in the tropics are probably related to different levels of smoothing in the two GPS-RO datasets.

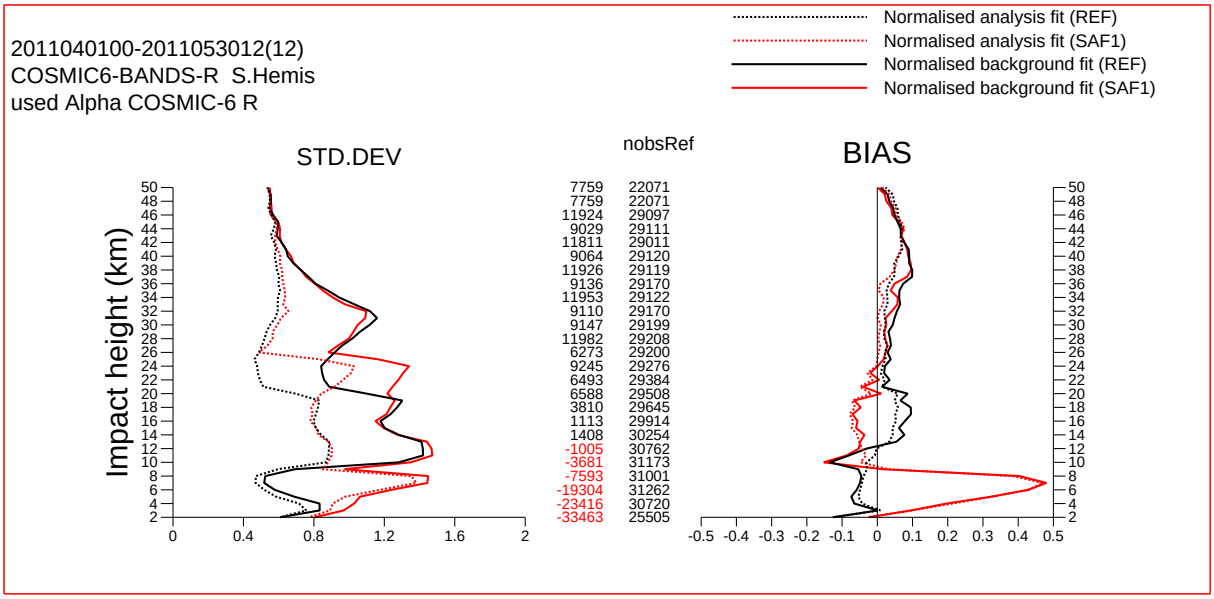

Figure 1.7: The noise normalised forecast and analysis departure statistics ((o-b)/σ_o and (o-a)/σ_o) for COSMIC-6 rising measurements in the southern hemisphere, for the REF (black line) and SAF1 (red line) experiments. The statistics are computed for the period April 1 to May 30, 2011. The central columns give the data numbers. The right hand column "nobsREF" refers to the number of bending angles in 1 km vertical bins used in the REF experiment. The other column gives the difference in the number of binned bending angles used in the two experiments (REF-SAF1). Red indicates that the REF experiment has lower data numbers.

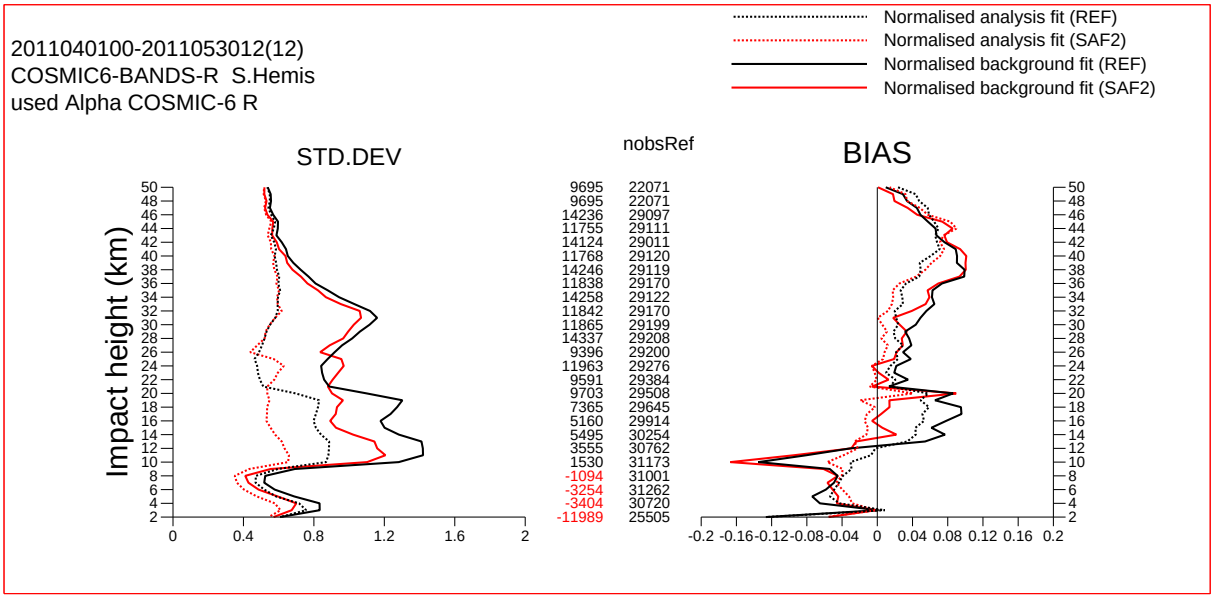

Figure 1.8: As Figure 1.7 but using the SAF2 data.

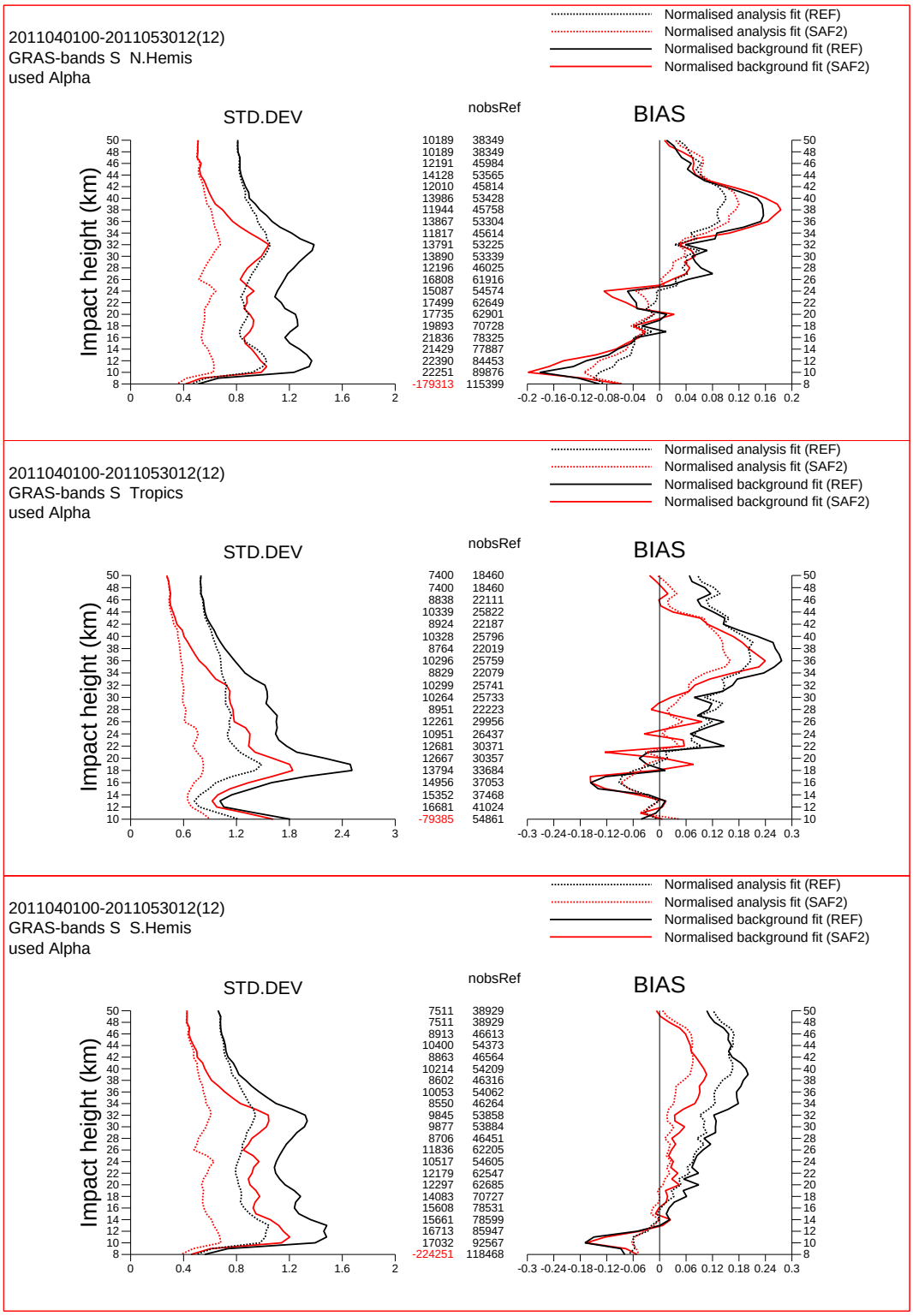

Figure 1.9: The noise normalised forecast and analysis departure statistics ((o-b)/σ_o and (o-a)/σ_o) for GRAS setting measurements for the REF (black line) and SAF2 (red line) experiments. The statistics are computed for the period April 1 to May 30, 2011. The central columns give the data numbers. The GRAS data numbers in the REF experiment are higher.

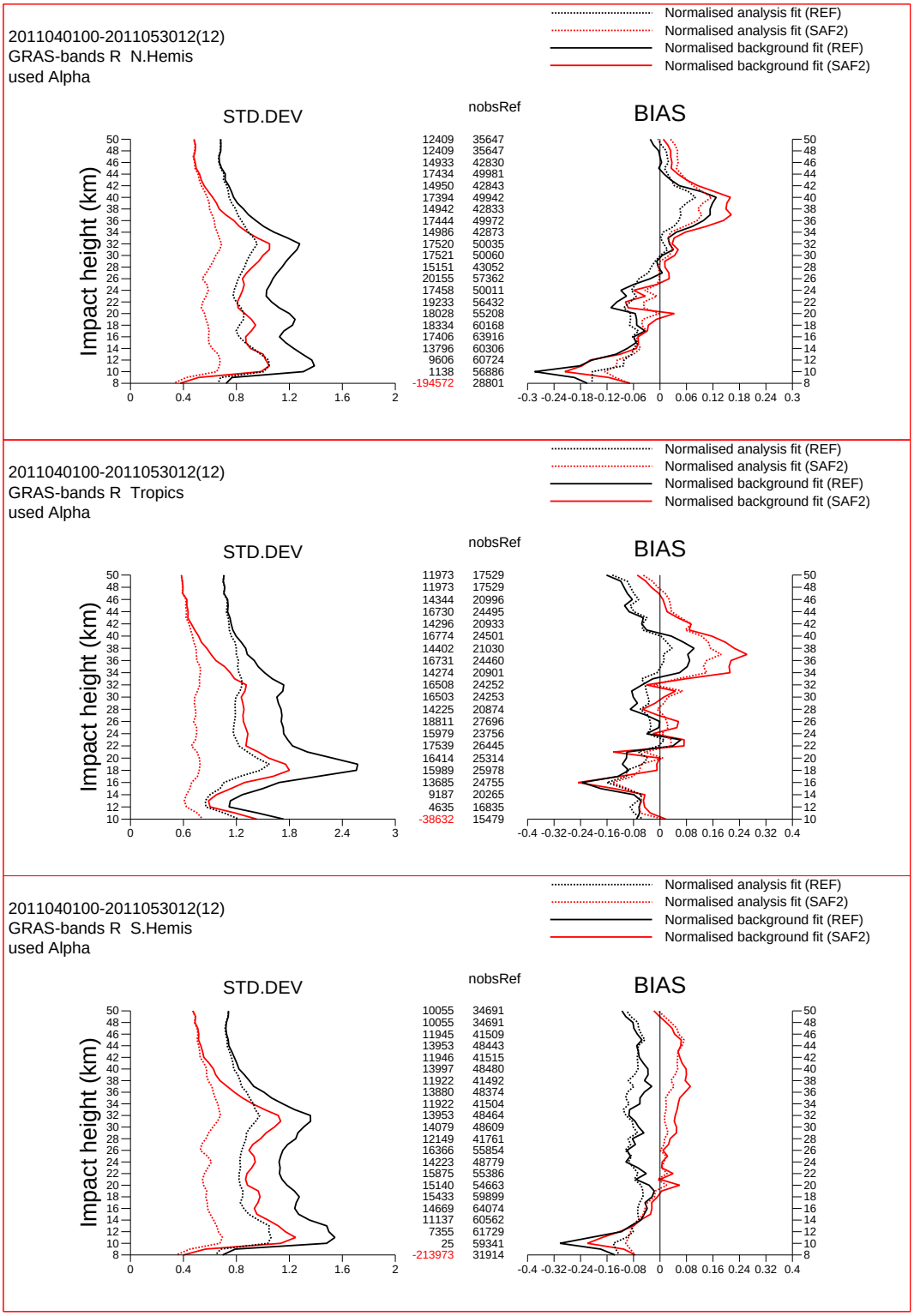

Figure 1.10: As Figure 1.9 but for rising data.

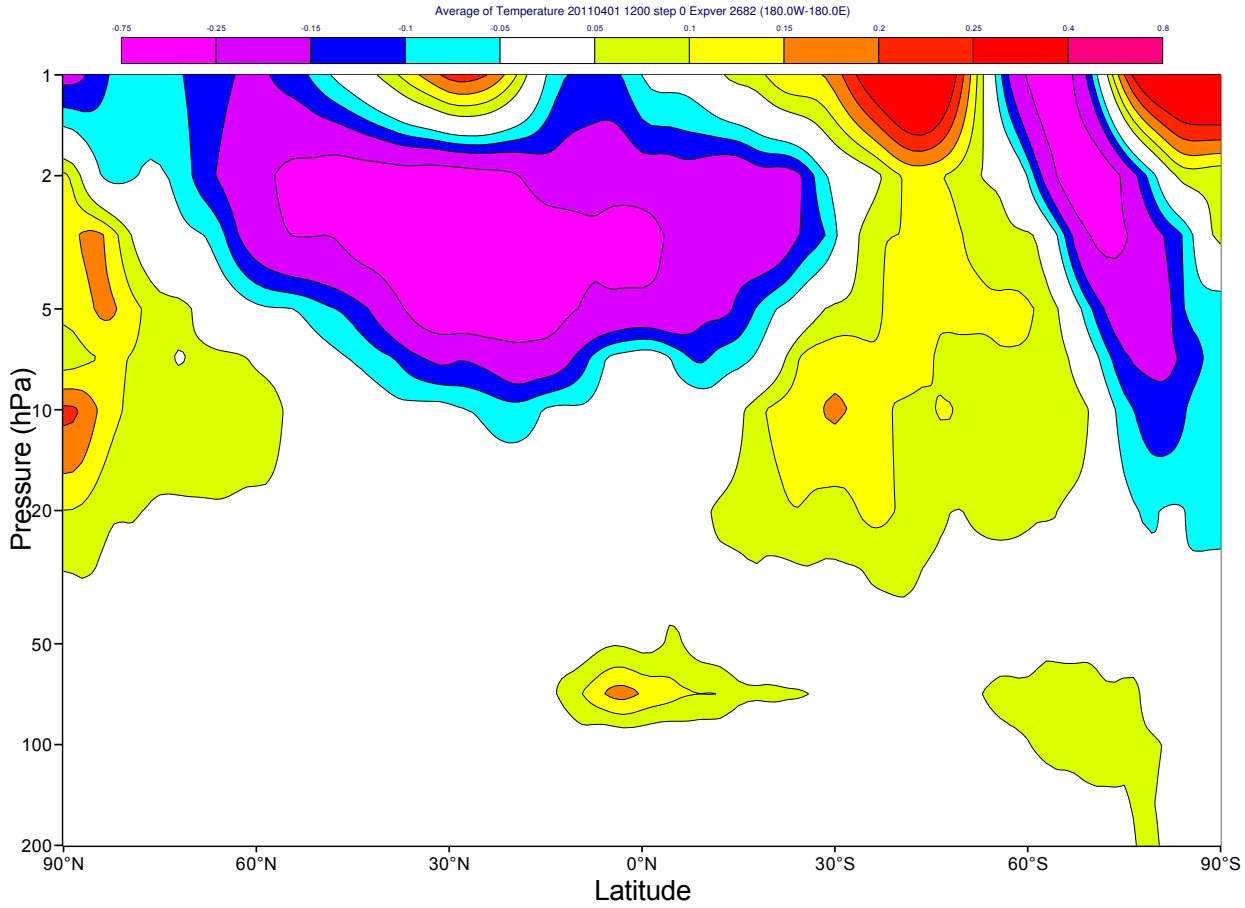

Figure 1.11: As Figure 1.2 but computing the (REF-SAF2) mean temperature differences for the period April 1 to May 30, 2011.

2 Summary and Future Work

The purpose of this study has been to compare different reprocessed GPS-RO datasets within a Copernicus ERA-5 climate reanalysis system, and select datasets to be used in the two planned ROM SAF reanalyses. We have tested two reprocessed datasets provided by the ROM SAF, a reprocessed dataset provided by UCAR, and the operational data available during this period. We were not able to test reprocessed data provided by EUMETSAT because it was not available during 2016.

A key result has been the importance of AMSU-A channel 14 radiances for constraining a known model bias in the upper stratosphere and mesosphere, where the GPS-RO information content falls rapidly. The model bias seems to be particularly problematic in the southern polar region for the period tested here, and it appears be in the GPS-RO null-space. Consequently, we suggest that channel 14 should be included in both of the planned reanalyses, because it clearly complements the GPS-RO.

The other key results can be summarised as follows:

1. The differences in the mean bending angle departure statistics are typically $\sim 0.1\%$ in the vertical interval between 10-30 km.
2. The globally averaged mean temperatures below 5 hPa seem to be quite insensitive to the differences in the GPS-RO datasets.
3. The departure statistics of the SAF2 dataset are clearly superior to the SAF1 dataset, as a result of setting the QC flags correctly in the SAF2 data.
4. Both ROM SAF datasets tend to have lower data numbers than either the operational datasets or the reprocessed data provided by UCAR. However, the reasons are understood and they will be corrected in the official “ROM SAF CDR V1.0” reprocessing.

The next phase of this work will be to perform the ROM SAF reanalyses for the 2007-2015 period. We currently plan to use the ROM SAF CDR V1.0 reprocessing, although it should be noted that we have not investigated ROM SAF Metop-B GRAS data here. In addition, a short experiment with the official ROM SAF CDR V1.0 for the period considered here is probably necessary, before starting the long reanalysis, to confirm that no new errors have been introduced in the ROM SAF reprocessing, and confirm that the ROM SAF data numbers have increased.

Acknowledgments

We would like to acknowledge input from the ROM SAF team, including Hans Gleisner, Stig Syndergaard and Kent Lauritsen.

References

Ao, C. O., A. J. Mannucci, and E. R. Kursinski, 2012: Improving GPS Radio occultation stratospheric refractivity retrievals for climate benchmarking. *Geophys. Res. Lett.*, **39**, L12701,doi:10.1029/2012GL051720.

Aparicio, J. M., and G. Deblonde, 2008: Impact of the assimilation of CHAMP refractivity profiles in Environment Canada global forecasts. *Mon. Wea. Rev.*, **136**, 257–275.

Cucurull, L., J. C. Derber, R. Treadon, and R. J. Purser, 2007: Assimilation of Global Positioning System Radio Occultation Observations into NCEP's Global Data Assimilation System. *Mon. Wea. Rev.*, **135**, 3174–3193.

Gleisner, H., and S. B. Healy, 2013: A simplified approach for generating GNSS radio occultation refractivity climatologies. *Atmos. Meas. Tech.*, **6**, 121–129.

Healy, S. B., 2001: Smoothing radio occultation bending angles above 40 km. *Ann. Geophys.*, **19**, 459–468.

Healy, S. B., 2011: Refractivity coefficients used in the assimilation of GPS radio occultation measurements. *J. Geophys. Res.*, **116**, doi:10.1029/2010JD014013.

Healy, S. B., and J.-N. Thépaut, 2006: Assimilation experiments with CHAMP GPS radio occultation measurements. *Q. J. R. Meteorol. Soc.*, **132**, 605–623.

Kursinski, E. R., G. A. Hajj, J. T. Schofield, R. P. Linfield, and K. R. Hardy, 1997: Observing earth's atmosphere with radio occultation measurements using the Global Positioning System. *J. Geophys. Res.*, **102**, 23.429–23.465.

Leroy, S. S., J. G. Anderson, and J. A. Dykema, 2006: Testing climate models using GPS radio occultation: A sensitivity analysis. *J. Geophys. Res.*, **111**, D17105,doi:10.1029/2005JD006145.

Leroy, S. S., C. O. Ao, and O. Verkhoglyadova, 2012: Mapping GPS Radio Occultation Data by Bayesian Interpolation. *J. Atmos. Oceanic Tech.*, **29**, 1062–1074, DOI: 10.1175/JTECH–D–11–00179.1.

Poli, P., S. B. Healy, and D. P. Dee, 2010: Assimilation of Global Positioning System radio occultation data in the ECMWF ERA-interim reanalysis. *Q. J. R. Meteorol. Soc.*, **136**, 1972–1990. doi: 10.1002/qj.722.

Poli, P., P. Moll, D. Puech, F. Rabier, and S. B. Healy, 2009: Quality control, error analysis, and impact assessment of FORMOSAT-3/COSMIC in numerical weather prediction. *Terr. Atmos. Ocean*, **20**, 101–113.

Rabier, F., H. Järvinen, E. Klinker, J.-J. Mahfouf, and A. J. Simmons, 2000: The ECMWF operational implementation of four dimensional variational assimilation. Part I: Experimental results with simplified physics. *Q. J. R. Meteorol. Soc.*, **126**, 1143–1170.

Rennie, M. P., 2010: The impact of GPS radio occultation assimilation at the Met Office. *Q. J. R. Meteorol. Soc.*, **136**, 116–131.doi: 10.1002/qj.521.

Steiner, A. K., D. Hunt, S.-P. Ho, G. Kirchengast, A. J. Mannucci, B. Scherllin-Pirscher, H. Gleisner, A. von Engeln, T. Schmidt, C. Ao, S. S. Leroy, E. R. Kursinski, U. Foelsche, M. Gorbunov, S. Heise, Y.-H. Kuo, K. B. Lauritsen, C. Marquardt, C. Rocken, W. Schreiner, S. Sokolovskiy, S. Syndergaard, and J. Wickert, 2013: Quantification of structural uncertainty in climate data records from GPS radio occultation. *Atmos. Chem. Phys.*, **13**,

1469–1484.

ROM SAF (and GRAS SAF) Reports

SAF/GRAS/METO/REP/GSR/001	Mono-dimensional thinning for GPS Radio Occulation
SAF/GRAS/METO/REP/GSR/002	Geodesy calculations in ROPP
SAF/GRAS/METO/REP/GSR/003	ROPP minimiser - minROPP
SAF/GRAS/METO/REP/GSR/004	Error function calculation in ROPP
SAF/GRAS/METO/REP/GSR/005	Refractivity calculations in ROPP
SAF/GRAS/METO/REP/GSR/006	Levenberg-Marquardt minimisation in ROPP
SAF/GRAS/METO/REP/GSR/007	Abel integral calculations in ROPP
SAF/GRAS/METO/REP/GSR/008	ROPP thinner algorithm
SAF/GRAS/METO/REP/GSR/009	Refractivity coefficients used in the assimilation of GPS radio occultation measurements
SAF/GRAS/METO/REP/GSR/010	Latitudinal Binning and Area-Weighted Averaging of Irregularly Distributed Radio Occultation Data
SAF/GRAS/METO/REP/GSR/011	ROPP 1dVar validation
SAF/GRAS/METO/REP/GSR/012	Assimilation of Global Positioning System Radio Occultation Data in the ECMWF ERA-Interim Re-analysis
SAF/GRAS/METO/REP/GSR/013	ROPP PP validation
SAF/ROM/METO/REP/RSR/014	A review of the geodesy calculations in ROPP
SAF/ROM/METO/REP/RSR/015	Improvements to the ROPP refractivity and bending angle operators
SAF/ROM/METO/REP/RSR/016	Simplifying EGM96 Undulation calculations in ROPP
SAF/ROM/METO/REP/RSR/017	Simulation of L1 and L2 bending angles with a model ionosphere
SAF/ROM/METO/REP/RSR/018	Single Frequency Radio Occultation Retrievals: Impact on Numerical Weather Prediction
SAF/ROM/METO/REP/RSR/019	Implementation of the ROPP two-dimensional bending angle observation operator in an NWP system
SAF/ROM/METO/REP/RSR/020	Interpolation artefact in ECMWF monthly standard deviation plots
SAF/ROM/METO/REP/RSR/021	5th ROM SAF User Workshop on Applications of GPS radio occultation measurements
SAF/ROM/METO/REP/RSR/022	The use of the GPS radio occultation reflection flag for NWP applications
SAF/ROM/METO/REP/RSR/023	Assessment of a potential reflection flag product
SAF/ROM/METO/REP/RSR/024	The calculation of planetary boundary layer heights in ROPP
SAF/ROM/METO/REP/RSR/025	Survey on user requirements for ionospheric products
SAF/ROM/METO/REP/RSR/026	Estimates of GNSS radio occultation bending angle and refractivity error statistics
SAF/ROM/METO/REP/RSR/027	Recent forecast impact experiments with GPS radio occultation measurements

ROM SAF Reports are accessible via the ROM SAF website: http://www.romsaf.org